Controlling catalytic activity of gold cluster on MgO thin film for water splitting

Zijing Ding,[1,2] Lei Yan,[1] Zi Li,[3] Wei Ma,[4] Gang Lu,[2,*] and Sheng Meng[1,†]

[1]*Beijing National Laboratory for Condensed Matter Physics and Institute of Physics, Chinese Academy of Sciences, Beijing 100190, China*
[2]*Department of Physics and Astronomy, California State University Northridge, Northridge, California 91330, USA*
[3]*Institute of Applied Physics and Computational Mathematics, Beijing 100088, China*
[4]*Ningxia Key Laboratory of Photovoltaic Materials, Ningxia University, Yinchuan 750021, China*

We propose that supported gold clusters on MgO thin film can potentially serve as an efficient photocatalyst for water splitting. The catalytic activity of the gold cluster is enhanced by excess electrons occupying its quantum well states (QWSs) and can be controlled by varying the oxide thickness, introducing defects/doping in the substrate, and modulating the plasmonic response of the Au cluster. We find that the bonding between the water molecule and certain QWSs can significantly reduce the water splitting energy barrier in its ground state. More importantly, the water splitting is nearly spontaneous when the QWS is photoexcited. First-principles real-time electron dynamics simulations reveal that the excited QWS in the supported gold cluster has a long lifetime on the scale of picoseconds. Generation of activated hydrogen atoms is predicted to occur spontaneously following photoexcitation, and the yield of H_2 gas is maintained by enriching hydrogen concentration without poisoning the catalyst. These results illustrate promising routes for promoting photocatalysis via engineering the energy levels of supported metal clusters.

I. INTRODUCTION

Water photosplitting has attracted a great deal of attention recently owing to its potential impacts on diverse research fields such as catalysis, water decontamination, and clean energy, to name but a few. Current systems for efficient water photosplitting are mostly based on semiconductor materials such as TiO_2 [1], ZnO [2], GaN:ZnO solid solution [3], and $BiVO_4$ [4], etc. Despite the tantalizing potentials, these materials suffer from problems of either low visible light absorption or structural instability in aqueous solutions under intense solar irradiation. To partially alleviate the problems, insulating oxides, such as MgO, have also been studied recently; they possess simple crystallographic structures and more importantly, are durable against harsh environments. However, although water molecules can dissociate easily on ultrathin MgO films [5], the final product is primarily hydroxyl, which cannot be directly used for energy applications. Furthermore, the wide energy gaps limit the sunlight absorption, which provides energy input for the reactions.

Metal clusters supported on oxide insulators are stable and widely used as active catalytic centers for chemical reactions, including CO oxidation [6–8], acetylene hydrochlorination [9–11], and water-gas-shift reactions [12]. Thanks to drastic field enhancements and easy tunability of plasmon excitations [13,14], photocatalysis utilizing plasmonic metal structures becomes particularly attractive. For instance, gold nanoparticles supported on titania exhibit photocatalytic activity for water splitting under UV, visible, and near-infrared light [15–17]. Dramatic enhancement of photocurrent for water splitting under visible light has been reported upon Au thin-film deposition on TiO_2, which is attributed to local field effects rather than the commonly assumed electron transfer mechanism [16]. Plasmon excitation of Ag nanocubes couples strongly to thermal energy to facilitate O_2 dissociation at low temperatures [13]. Overall, metal clusters on oxides can enhance sunlight absorption and exhibit high photocatalytic activity. Therefore, it is of both scientific and technological importance to explore the fundamental physics underlying the alternative platform for water photosplitting, which utilizes the quantum effects of supported metal clusters on photoinactive wide-gap oxide substrates.

Fortunately, atomic structures of gold clusters supported on MgO thin film, dependent on the cluster size and the substrate, have been investigated by *in situ* scanning tunneling microscopy (STM). Other properties, including molecular adsorption [18], electronic structures [19], and optical absorption [20], were also reported by combined STM and numerical simulations. CO oxidation catalyzed by gold clusters on MgO thin film supported on Mo(100) surface was investigated in great detail [7,21]. Owing to confinement effects, the gold clusters exhibit several quantum well states (QWSs), and visible light excitation enables hot electrons to jump into higher energy levels of QWSs [20]. However, the catalytic reactivity of gold clusters supported on MgO towards water splitting, especially upon photoexcitation, is rarely investigated, either experimentally or theoretically. In this paper, we strive to fill this gap by providing a comprehensive picture of the underlying physical processes from first-principles calculations.

To examine whether the gold cluster on the MgO surface is a suitable catalyst for water photosplitting to produce H_2, we need to understand the mechanism for the photocatalytic reactions on the gold clusters. Hot electrons from the gold cluster excited by visible light were found to facilitate water splitting, because their energy levels are much higher than the standard hydrogen potential [20]. In this work, the dynamics and mechanism of water photosplitting catalyzed by the gold cluster are investigated. In contrast to the reaction on bare oxide insulators, water dissociates into activated H atoms upon supported gold clusters. The catalytic activity of the gold cluster is enhanced by the excess electrons in the QWS, which

---

*Corresponding author: ganglu@csun.edu
†Corresponding author: smeng@iphy.ac.cn

can be controlled by the substrate thickness, the presence of defects/doping in the substrate, and plasmonic excitations of the gold cluster. By tuning these parameters, one can reduce the energy barriers for water splitting dramatically. In addition, our calculations confirm that the gold cluster is not poisoned during the water splitting process and could collect multiple hydrogen atoms, which is key to successful H_2 production.

II. METHODS

First-principles calculations are performed within the framework of density functional theory (DFT) [22] and constrained DFT. Ground-state (GS) geometries have been optimized using projector augmented wave pseudopotentials [23,24] and the Perdew-Burke-Ernzerhof [25] form for exchange-correlation functional, as implemented in the Vienna *ab initio* simulation package (VASP) [26]. The substrate consists of two monolayers (2ML) of MgO thin film, in registry with three Ag(001) atomic planes with a lattice constant of 4.09 Å, taken from experiments. A Ag(6 × 6) surface unit cell is constructed to hold a Au_8 cluster and adjacent water molecules.

Transition states for water splitting are obtained using the climbing image nudged elastic band (NEB) method [27]. In excited states, the barriers of reaction paths for the ground state are calculated using the constrained DFT, where QWS occupations are fixed to some predetermined values characterizing the reaction paths. In this way, the excitation energies along the reaction paths can be extracted. NEB calculation within the constrained DFT is not yet available due to inaccurate force calculations. For simplicity, we calculate the excitation energy of the individual configurations along the reaction pathway, which was estimated from the ground-state calculations. The barriers obtained from these nonoptimized pathways thus represent an upper limit of the reaction barriers upon photoexcitation. Due to the current limitation of DFT simulation, we cannot find saddle points in the excited states, while in the GS pathways we may miss the structures for the saddle points, which correspond to a higher barrier in the excited states. Increasing the number of the middle-point states could reduce the error but cannot ultimately eliminate the error, unfortunately. Besides this error in identifying the correct pathway for photoexcited reactions, the accuracy in energy barriers calculated by constrained DFT itself is also limited.

The lifetime of excited states is computed using nonadiabatic molecular dynamics [28,29] combined with the fewest switches surface-hopping (FSSH) approach [30,31]. To be specific, the wave function of excited states is expanded in the basis of adiabatic Kohn-Sham (KS) orbitals with expansion coefficient determined by the time-dependent DFT equation. Based on the expansion coefficient, one can determine the electron transition rates following surface-hopping dynamics, where the excited electron is assumed to stay in one adiabatic KS state at a time, but it can hop from one state to another. The hopping probability can be determined from the expansion coefficient [28–31]. Here, we employ a simplified surface-hopping method, where the hop rejection in the traditional FSSH method is replaced by multiplying the hop probability with the Boltzmann factor for the energetic upward transitions [28,29]. To capture the stochastic nature of the coupled electron-ion dynamics, 100 short nonadiabatic electronic state evolution trajectories are averaged to determine the electron hopping rate (or lifetime).

III. RESULTS AND DISCUSSION

A. Water adsorption

Adsorption geometries, electronic structures, and excited-state properties of gold clusters depend on the size of gold clusters and substrate. Gold cluster Au_8 is more stable than other sizes of Au_n ($2 \leqslant n \leqslant 25$), which is a two-dimensional (2D) structure irrespective of whether in vacuum or on MgO/Ag(001) [19,32,33]. The adsorption configuration of a water molecule on Au_8/MgO/Ag(001) is shown in Fig. 1(a). The water molecule would sit on the top of magnesium atoms which are closest to the gold cluster [20,34–36], with the OH bond pointing to the gold cluster. All adsorption sites are considered, which are denoted by red semitransparent circles in Fig. 1(b). The adsorption energies of the water molecule on these sites are in the range of 0.65–0.80 eV, and the most
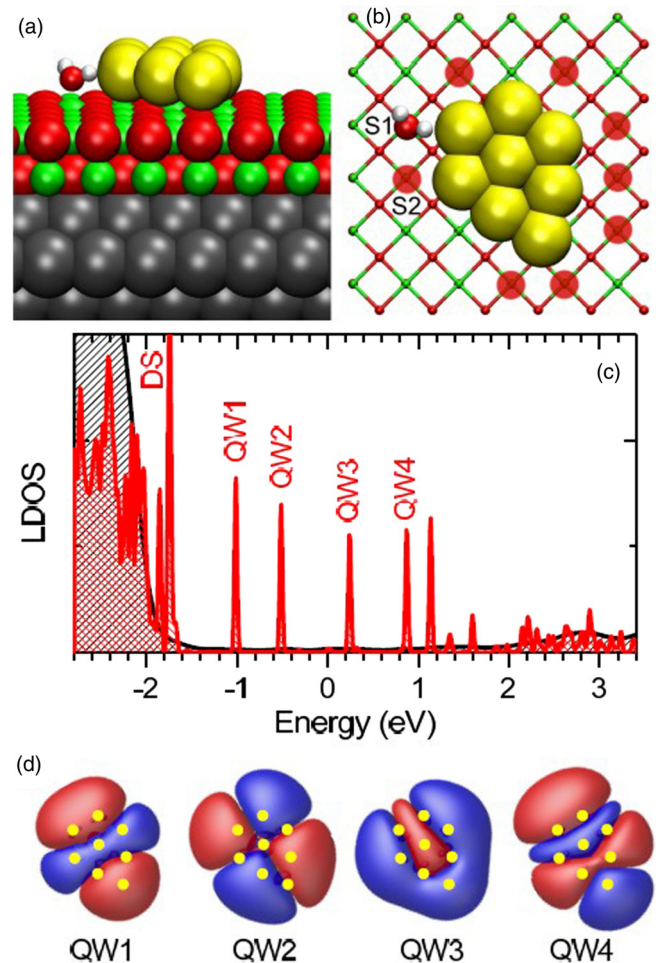

FIG. 1. (a,b) Side and top views of the optimized configuration of H_2O on Au_8/MgO(2ML)/Ag(001). Green, red, yellow, white, and gray spheres represent Mg, O, Au, H, and Ag atoms, respectively. Red semitransparent circles show all the water adsorption sites. (c) Local DOS of the gold cluster (in red) and MgO thin film (in black). (d) Wave functions of four QWSs, QW1–QW4. Yellow dots indicate the position of the gold atoms.

stable adsorption site is the S1 site. Thanks to the symmetry of Au_8, all the energy differences between two symmetrical sites are smaller than 0.02 eV. All the binding sites are more stable than those on clean MgO(100) with an adsorption energy of 0.42 eV. In contrast, the water molecule does not directly adsorb onto the top site of the Au cluster, whose adsorption energy is below 0.13 eV [20].

Local density of states (LDOS) of Au_8 on MgO(2ML)/Ag(001) is shown in Fig. 1(c). The energy levels of the gold cluster's QWSs, QW1–QW4, are in the gap of MgO thin film, which is about $-2.0 \sim 2.0$ eV in our calculations. The wave functions of these QWSs in vacuum are shown in Fig. 1(d). The Fermi level of this system, $E_f = 0$, is fixed by the silver substrate. The energy level of $5d$-orbital states (DS) of Au_8 overlaps with the valence band of the MgO thin film.

We find that one of the OH bonds for the water molecule on the S1 site points to the antinode of QW2, which is the highest occupied molecular orbital (HOMO) of Au_8, while the bond of the water molecule on site S2 points towards the node of QW2. Therefore, the water molecule on site S1 is more stable than that on S2, and both sites are carefully considered for comparison in the following. The lowest unoccupied molecular orbital (LUMO) of Au_8, QW3, is also crucial to investigate the photoexcitation processes. Contrary to the interaction with QW2, H_2O on sites S1 and S2 points to the node and antinode of QW3, respectively. Therefore, all the adsorption sites can be divided into two types of adsorption sites, exemplified by S1 and S2.

B. Water splitting pathway

We further investigate the ground-state kinetics of water dissociation on Au_8/MgO(2ML)/Ag(001) to produce activated hydrogen atoms (denoted [H]). The reaction energies are shown in Fig. 2. We take the S1 adsorption site, for example. The water dissociation reaction starts with an intact water molecule adsorption (A). The attraction between H_2O and the QWS orients the OH bond of the water molecule pointing to the gold atoms with H-Au length of $\sim$2.3 Å. The dissociative (D) adsorption is the reaction product: the OH group binds onto the bridge site of the Mg-Mg bond on the MgO surface, and the hydrogen atom binds on the gold cluster. The equilibrium distance between the [H] and the nearest Au atom is $\sim$1.6 Å. Bader analysis [37] reveals that the charge on the adsorbed OH is $\sim -0.85e$, and that on [H] is $-0.04 \sim -0.12e$. That is, the reaction product OH is anionic while the [H] is neutral (the extra electron comes from the Ag substrate).

In comparison, the H atom binding with the O atom of the MgO surface is one of the products of water dissociation on MgO/Ag(001) without the gold cluster. Unlike water dissociation catalyzed by the gold cluster, the H atom is similar to that in a water molecule and is inactive, since the charge of H atom therein is $+0.57e$ [38]. We find that electron transfer from the silver substrate to the coupled Au_8-OH species results in one excess electron. During water dissociation, the transition (T) state is obtained by the NEB calculations. In the T state, the OH bond in the water molecule is broken and stays in its original site. The OH bond in the T state is only $\sim$0.84 Å away from that in the D state.
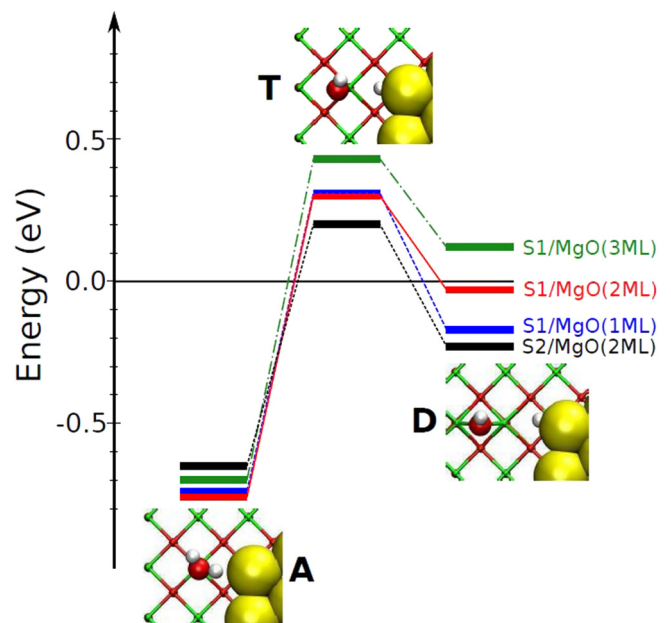

FIG. 2. Reaction energy profiles and structures of water dissociation on Au_8/MgO/Ag(001) for the adsorption sites (S1, S2) and 1–3 ML MgO thin film.

Motivated by a recent work where the water splitting barrier depends sensitively on the thickness of MgO thin film [33], we first look at whether it also applies to the catalytic activity of supported gold clusters (Fig. 2). With MgO thickness ranging from 1 to 3 ML, the activation energy (E_a) for water dissociation increases from 1.05 to 1.13 eV upon water adsorption on the S1 site, and the reaction heat $\Delta E = E_D - E_A$, namely, the energy needed for water splitting, ascends from 0.42 to 1.00 eV. Unlike water dissociation on bare MgO/Ag(001) [39], decreasing the MgO thickness has a minor influence on the water splitting barrier with the supported gold clusters. The results are comparable with the barriers in the same reaction path using the DFT+U method with $U = 5.0$ eV. For water dissociation on site S1 with 2 ML MgO, the barrier calculated using GGA+U is 1.12 eV, quite close to that without the U-term correction, implying that the on-site correlation is not important during water dissociation.

On the other hand, we find that the adsorption sites have significant influences on the barriers of water dissociation. For different adsorption sites [Fig. 1(b)], E_a for water dissociation varies from 0.85 to 1.33 eV. The energy difference $E_T - E_D$, caused by the OH moving away from Au_8 to its optimal position, is 0.33–0.44 eV for all sites. The lowest barrier, 0.85 eV, corresponds to water dissociation on site S2 (Fig. 2). However, this minimum barrier is still higher than 0.77 eV, which is the barrier for water dissociation on MgO(2ML)/Ag(001) without the gold cluster [5]. The hydroxylated MgO surface, which is the product of water dissociation without the gold cluster, is generated more easily than the activated hydrogen from water splitting catalyzed by Au_8. However, the hydroxylated MgO surface cannot produce H_2 easily. In reality, H_2 production can be achieved under the conditions of a low water coverage and a high temperature, facilitating preferable water adsorption and

splitting at the vicinity of gold clusters [40], or on the fully hydroxylated MgO surface.

To explain the trend in reaction barriers, the binding energy of [H] on Au_8, which depends on the interactions between the [H] and QWSs, is in the range of $-0.12 \sim 0.43$ eV [41]. The largest binding energy for [H]-Au_8 is related to the lowest barrier for water dissociation, since large binding energies enable the H atom to overcome the split energy of the OH bond and reduce the barriers. Therefore, the difference in energy barriers depends on the interaction between the [H] and QWSs of the gold cluster in the T state.

Furthermore, we note that the Coulomb interaction between OH^- and [H]-Au_8 is not the main reason behind the trend in reaction barriers. Since there is more charge transfer from the substrate to the [H]-Au_8 complex on the other sites (-2.11 to $-2.53e$) than on S1 site ($-1.65e$), the Coulomb attraction on other sites would be stronger than that on the S1 site. However, both E_D and E_a on the S1 site are neither the highest nor the lowest. In other words, there is no direct correlation between the Coulomb interaction of reaction products and the energy barrier for water dissociation.

C. Tuning barriers by substrate doping

Different from tuning MgO thickness, burying defects into the MgO surface to increase the doping level is a much more effective way to control the QWS occupation of the gold cluster. We then construct a 5-ML (6×6) MgO(100) substrate with several defects but no silver layers underneath. Burying negative defects into the MgO surface, such as using aluminum to substitute magnesium (Al_{sub}) or burying oxygen vacancy (O_{vac}), could provide excess electrons (see Table I). The excess electrons would transfer from the substrate to Au_8, making the higher level of QWSs (QW2, etc.) occupied, similar to the case of MgO thin film on silver substrate. Furthermore, with more electrons transfer to Au_8, the QW3 state could be partially occupied.

On a perfect MgO(100) substrate without any defect, the QW1 state is the HOMO of Au_8 while the QW2 is the LUMO. The barrier of water splitting in this case ranges from 2.23 eV (on site S1) to 1.94 eV (on site S2). In addition, OH binds strongly to the gold cluster and cannot diffuse away. As a result, efficient water splitting cannot be achieved. The barriers
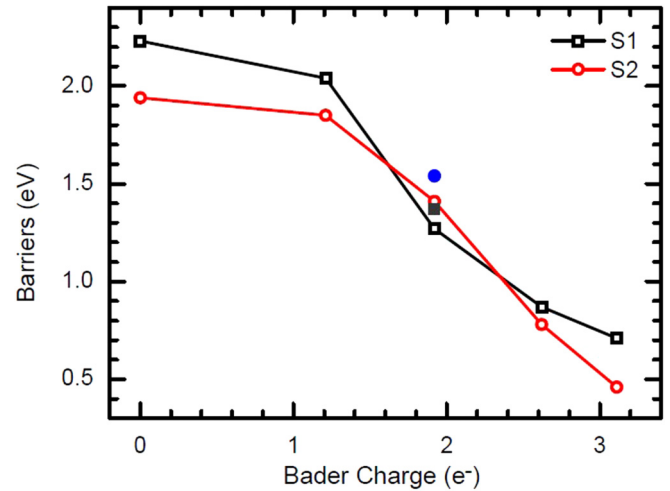

FIG. 3. Barriers of water dissociation as a function of excess electrons of Au_8 controlled by several buried defects for water molecules on S1 (squares) and S2 (circles) sites. The data for buried Al_{sub} defects are shown in open squares (S1)/circles (S2) and for the O_{vac} defects in filled square (S1)/circle (S2).

of water dissociation catalyzed by Au_8 on MgO(100) with several defects are shown in Fig. 3. With burying $1-4$ Al_{sub} defects randomly into the substrate, the excess electrons of the gold cluster increase from 0 to $3.11e$. More strikingly, as the QW2 and QW3 are occupied, E_a drops from 2.23 to 0.46 eV.

The occupied QW2 is induced by burying two Al_{sub} defects (~ 0.75 wt %) or an O_{vac} defect in the MgO. The barrier for water dissociation with an O_{vac} defect, which is 1.37 eV on the S1 site and 1.54 eV on the S2 site, is significantly reduced compared to that on the defect-free MgO substrate. The wave function of QW2 distributes around the [H] binding site with the gold cluster and thus promotes the OH bond splitting because of the stronger σ bond between the [H] and QW2. The attraction of the O_{vac} defect for electrons is stronger than that of the Al_{sub} defects; therefore E_a on Au_8/MgO(100) with O_{vac} is a little higher than that with $2Al_{sub}$. Due to the unoccupied QW3 during the reaction, E_a on site S2 is higher than that on site S1.

With higher QWS levels occupied, the water splitting barrier is further decreased, thanks to the bonding between the dissociated H product and the excess occupied QWS. For instance, inserting $4Al_{sub}$ defects (~ 1.5 wt %) in the supercell makes the QW3 partly occupied. The barrier for water dissociation is further reduced to 0.71 eV on S1 and 0.46 eV on the S2 site. Without QW3 occupied, [H] on the S2 site interacts weakly with Au_8 due to the presence of the node of QW2, resulting in an unstable transition state and a high energy barrier. With the occupied QW3, [H] on the S2 site interacts strongly with QW3 owing to its wave-function antinode around the S2 site, significantly reducing the energy barrier from 1.94 to 0.46 eV. Therefore, with more electrons transferring from defective MgO to Au_8, the partially occupied QW3 promotes water splitting significantly.

These results reveal the significance of the substrate in controlling the occupation of the gold cluster's QWSs: tuning the defect concentration could help to control the catalytic

TABLE I. Bader charge analysis in A states (Q_A), the HOMO of Au_8, and energy barriers (E_a) of water dissociation on the S1 and S2 sites with different substrates.

Substrates	$Q_A(|e|)$	HOMO	S1	S2
MgO(1ML)/Ag(100)	-2.12	QW2	1.05	0.85
MgO(2ML)/Ag(100)	-1.89	QW2	1.06	0.85
MgO(3ML)/Ag(100)	-1.80	QW2	1.13	1.20
MgO(100)	0.00	QW1	2.23	1.94
MgO(100) with Al_{sub}	-1.21	QW2	2.04	1.85
MgO(100) with O_{vac}	-1.92	QW2	1.37	1.54
MgO(100) with $2Al_{sub}$	-1.92	QW2	1.27	1.41
MgO(100) with $3Al_{sub}$	-2.62	QW3	0.87	0.78
MgO(100) with $4Al_{sub}$	-3.11	QW3	0.71	0.46

activity of the metal clusters. We have demonstrated that adjusting the thickness (1–3 ML) of MgO film produces a less significant change in water dissociation barriers. Charge analysis indicates that the amount of charge transfer from the 1–3 ML MgO film to Au_8 barely varies in the range of $1.80 - 2.12e$. This interval of excess charges on Au_8 is very narrow by tuning the MgO thickness on Ag(001), while the interval of excess charges on Au_8 is wide by controlling the concentration of defects buried into the MgO substrate. The maximum charge of the gold cluster achieved is $-3.11e$, when MgO(100) is inserted with only $4Al_{sub}(1.5 wt\%)$ defects. In this case, the lowest barrier of 0.46 eV for water splitting is obtained on the S2 site. It is lower than 0.56 eV, which is the barrier needed for water dissociation on MgO(1ML)/Ag(001) without the gold cluster [5]. Consequently, water splitting on Au_8 is more efficient than on bare MgO ultrathin film, whose product is the activated [H] and hydroxylated MgO surface, respectively.

D. Barriers in excited states

Besides modifying the substrates, photoexcitation is another way to control the QWS occupation of the gold cluster. The photoexcited plasmon of a metal cluster decays either radiatively by emitting a photon or nonradiatively by generating an electron-hole pair [39]. Upon visible light excitation at the energy of 2.4–2.5 eV, higher QWS levels of the Au_8 cluster would be occupied [20]. The excitation generally comprises the contributions from DS to QW3, DS to QW4, and QW1 to QW4. The processes of water dissociation catalyzed by the excited Au_8 are calculated using constrained DFT, and the energy is obtained with the QWS occupation number fixed. The energy for water dissociation in the ground state and excited states on the S1/S2 site is shown in Fig. 4.

On the S1 site, the energy for the starting reactant configuration E_A in excited states (1.11–1.81 eV) is higher than that for the transition state E_T in the ground states (0.30 eV). The reaction barrier E_a in the excited states (0.82–0.97 eV) is lower than that in the ground state (1.08 eV). As the reaction paths are not optimized in the excited states, the real barriers are even lower than those listed in Table II. Although the excitation

TABLE II. Energy barriers for water dissociation on Au_8/(2ML)MgO/Ag(001).

Sites	S1	S2
Ground state	1.08	0.85
DS → QW3	0.97	0.17
DS → QW4	0.82	0.50
QW1 → QW4	0.95	0.78

QW1→QW4 has a great influence on water splitting, this excitation has a low fraction (<1%) in the visible light absorption [21]. Therefore, we can neglect this type of excitations.

In most cases, the reaction barriers in excited states are similar to their counterparts in the ground state. The excitation barriers on the S1 site are less than 1.0 eV and decrease a little (∼0.2 eV) because the binding energy between [H] and QW3 on site S1 is weak. Compared with the S1 site, the barriers for water splitting on site S2 are more sensitive to the excited states involved, due to the higher charge density of the QW3 on the S2 site. Among all cases investigated, water splitting on the S2 site with occupied QW3 has the lowest barrier of 0.17 eV [Fig. 4(b)]. This barrier is even lower than the zero-point energy (∼224 meV) of the asymmetric O-H stretching mode of H_2O, which is the main vibrational mode for water dissociation on MgO(100) [5]. Owing to the negligible E_a and the negative reaction heat $\Delta E = -0.1$ eV, the water splitting reaction is deemed spontaneous and exothermic on the S2 site via QW3.

The occupied QW3 has a significant impact on the reaction path. The reaction on S2 site in the ground state occurs from the A to T state via charge transfer with the QW3 occupied. Without charge transfer, the T state is the lowest energy state in the excited state (DS → QW3) because of the occupied QW3. Unlike other barriers, the reaction path is divided into two barriers by the original T state. The first one is ∼0.13 eV and the second is ∼0.5 eV, which reveals that the optimized configuration in the excited state is close to the T state. If the final state is trapped around the T state, the barrier could cross after deexcitation into the ground-state pathways. Otherwise, the reaction can proceed around the T state without trapping, and the barrier is about 0.17 eV to the D state. In either case, water dissociation is achievable almost spontaneously. With the occupied QW3 via doping of ∼1.5 wt % Al_{sub} defects into MgO substrate, more electrons on the gold cluster would result in larger Coulomb repulsion between OH^- and the cluster. For this reason, E_a in the excited state (0.17 eV) is even lower than the lowest one (0.46 eV) via doping.

Although it is not explicitly considered in this work, the plasmonic resonance of metallic nanoclusters depends sensitively on the size and shape of the clusters. The resonance in turn influences light absorption, hot electron generation, and field enhancement, all of which can be explored to enhance the catalytic activities. The proposed platform offers a fertile playground where these diverse physical phenomena can be integrated to yield alternative routes for water splitting.

FIG. 4. Reaction energy profiles of water dissociation in the ground state and the excited states of Au_8 on MgO(2ML)/Ag(001) when a water molecule is on the (a) S1 and (b) S2 site.

E. Estimate of excited-state lifetime

To rationalize the results of the excited-state energy barriers, we performed the first-principles surface-hopping calculations to estimate the lifetime of the excited states on the gold cluster
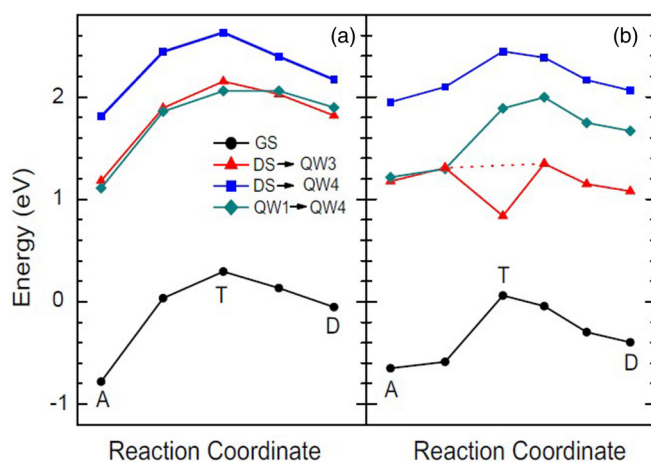
TABLE III. Lifetime (ps) of excited states (DS → QW3, DS → QW4, QW1 → QW4, QW1 → QW3) damping to unoccupied states (MgO, DS, QW1, QW3) of Au_8 on MgO(100) buried $2Al_{sub}$ defects. τ is the lifetime including all the decay channels of hot electrons. It is defined as $\tau^{-1} = \Sigma_i \tau_i^{-1}$, where τ_i is the lifetime of a single damping channel shown in the table. "–" denotes the impossible damping channel.

	MgO	DS	QW1	QW3	τ
DS → QW3	1.61	0.76	–	–	0.52
DS → QW4	1.16	0.98	–	3.96	0.47
QW1 → QW4	1.16	–	2.56	3.96	0.66
QW1 → QW3	1.61	–	0.76	–	0.52

(see Table III). Owing to charge transfer from substrate to the cluster Au_8, QW2 is occupied by two excess electrons [19,20] and does not participate in the excitation or degradation. The damping to the valence band of MgO has a small probability, since the entire hopping time is more than 1.1 ps. The transition from QW4 to QW3 with a hopping time of 3.96 ps is less possible. The lifetime of QW3 is 520 fs before decaying to the ground state. The lifetime of QW4 with DS unoccupied is 470 fs, by which ~88% damps to the ground state (530 fs) and ~12% damps to the QW3 (3960 fs). The lifetime of QW3 with QW1 unoccupied is ~520 fs. All of them are about 2 orders of magnitude longer than the periodicity of the asymmetric OH stretching mode of $H_2O(\nu_{OH} = 448$ meV, $\tau_{OH} = 9.2$ fs), which is the main vibrational mode leading to water splitting on MgO(100). In other words, the QWS lives long enough for the O-H stretching vibration to break the OH bond upon photoexcitation.

For a reaction barrier $E_a \leqslant 0.5$ eV, assuming a photon flux (Φ_0) of sunlight is typically 10^3 s^{-1} nm^{-2}, we estimate the reaction rate (η) at room temperature using the following equation:

$$\eta = \xi \, \Phi_0 \exp\left(-\frac{E_a - \frac{1}{2}\hbar\nu_{OH}}{kT} \right),$$

where the number of trials to break OH bond upon photoexcitation (ξ) is more than 50 per photon, $\frac{1}{2}\hbar\nu_{OH}$ is the zero-point energy (~0.22 eV), k is the Boltzmann constant, and the temperature (T) is 300 K. Thus the reaction rate is estimated to be >1.0/s per Au_8 site. However, for a metallic system like Au_7, the lifetime of the hot electron is too short to split water. Thus, the conclusion is not suitable for the metallic system.

F. Diffusion of reaction products

As a practical catalyst, the supported Au_8 on MgO should not suffer from poisoning and we performed the following simulations to establish this fact. First, we verify that the activated [H] can be readily collected on the Au_8. Both the barrier (~1.06 eV) and the reaction path of producing the second [H] on the S1 site are very close to that of producing the first [H] on the same site (~1.05 eV). The effect of [H] on the gold cluster is highly localized and has little influence on water dissociation on other distinct sites. Collecting the [H]s is not correlated with the adsorbed [H]s on the other sites. All the

reactions for [H] collection are similar to the production of first [H]. In the same mechanism of water dissociation, tuning the QWS occupation by defect doping and excitation is helpful for producing the [H]s.

In addition, we confirm that a neighboring water molecule hydrogen-bonded to the water molecule on the S1 site also enables efficient water dissociation, whose product [H] also could transport to Au_8. The reaction barrier on MgO bulk is 1.07 eV [5,38], close to water dissociation on the same site of Au_8 on MgO(2ML)/Ag(001). Therefore, water molecule adsorption does not have a negative effect on water dissociation, and the hydroxyl spreads away from the gold cluster, facilitating the separation of H and OH products.

We further simulate the diffusion of OH radical between two water molecules on MgO(2ML)/Ag(001) without the gold cluster. The simulation reveals that rapid proton transfer within the OH radical and water molecules could take place, similar to the proton transfer within water dimer and clusters [42]. The barrier is only 0.24 eV, smaller than 0.60 eV, which is the case without hydrogen bonds. With the hydrogen bond between water molecules, the OH radical spreads away from the gold cluster easily. We also find that the energy of OH removal $(E_T - E_D)$ is positively correlated with the MgO thickness [38].

Thanks to the significant overlap between DS states of the gold cluster and the valence bands of MgO surface, the hole in the DS states of Au_8 generated by photoexcitation would transfer to MgO very efficiently. The holes gathered on MgO substrate would oxidize OH groups generated from water dissociation and produce O_2 gas on MgO. In reality, MgO is a good hole conductor and is routinely used as an oxygen-storage material.

G. H_2 production

The activated [H] on the gold cluster can move easily between the different adsorption sites, with a barrier of 0.14 eV from the S1 to S2 site. The [H] on the S2 site is the most stable. It is likely that H_2 gas is produced by combining two and more activated hydrogen atoms on Au_8.

In order to confirm the possibility of hydrogen production on Au_8/MgO/Ag(001), we designed three reactant states (R) to synthesize hydrogen gas (H_2) as follows: (1) the dimer of OH belonging to the hydroxylated MgO surface without the gold cluster; (2) two [H]s adsorption on the neighboring sites of Au_8; and (3) H_2O and one [H] adsorption on the same site of Au_8. The structures of the reactants are shown in Fig. 5. Hydrogen production is performed to get the reaction product (P), which is a H_2 molecule weakly adsorbed on the MgO surface.

The transition states (T) and reaction paths are obtained by NEB calculations:

(1) When H_2 is synthesized from reactant state R_1: One hydrogen atom is split from surface hydroxyl and combines with the other H with a barrier of 1.83 eV. Because of the highest barrier, this reaction path is difficult to occur.

(2) From reactant state R_2: One [H] combines with another [H] with a barrier of 0.80 eV. Higher concentration of [H]s on Au_8 would result in an even lower barrier for H_2 desorption. Because ΔE is only ~0.1 eV, the energy of each hydrogen
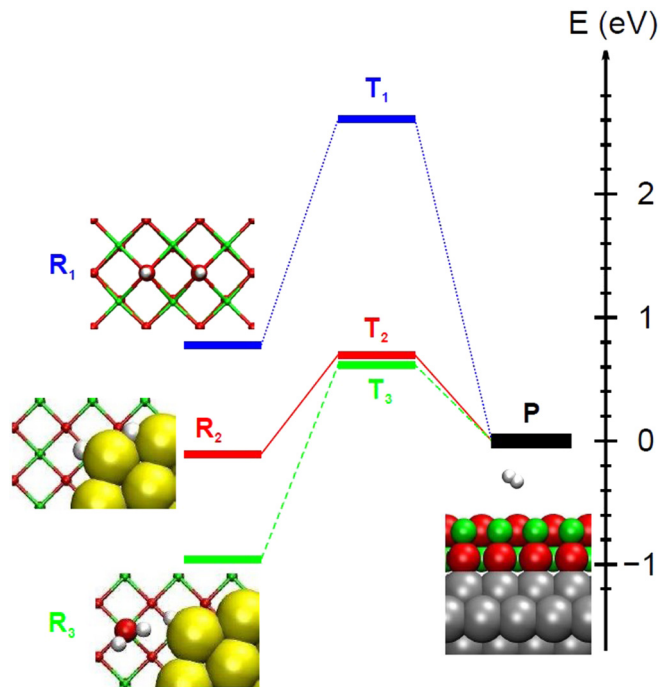
FIG. 5. Reaction energy profiles for H_2 generation on MgO(2ML)/Ag(001) without/with the gold cluster.

atom in the R_2 state is close to that of H_2. This barrier is the lowest, which is the most probable path for H_2 production.

(3) From reactant state R_3: The hydrogen atom splits from the water molecule and combines with the [H] on Au_8. The energy of transition state (T) is close to that of final state (P), which is determined by the repulsion between the H_2 molecule and the gold cluster. Because of the high stability of the reactant state (R) ($\Delta E = 0.96$ eV), the barrier 1.58 eV is so high that the reaction can hardly take place.

Without the gold cluster, hydrogen gas production is unlikely to occur on the bare MgO/Ag(001) surface owing to the large barriers. For the same reason, the dissociations of two water molecules on the same site are difficult for H_2 generation. The hydrogen gas is produced most possibly by

many activated hydrogen atoms on the same gold cluster. The gold cluster serves as a reaction center to collect activated hydrogen atoms and produce H_2 gas.

IV. CONCLUSION

In conclusion, our results demonstrate that Au_8 can be used as a catalyst to split water. The catalytic activity can be tuned by controlling the occupation of QWSs, especially the QW3, through the substrate effect, defect doping, and photoexcitation. In particular, water dissociation on the S2 site is spontaneous upon photoexcitation (DS $\rightarrow$ QW3), whose lifetime is long enough to split water efficiently. Both H and OH can diffuse easily without poisoning the catalyst. By combining many activated hydrogen atoms, H_2 gas is produced with a small barrier of less than 0.8 eV. We have discussed the cases of low coverage of water molecules above. For high coverage of water, we infer that the hydrogen-bond interaction would increase the polarizability of water molecules and accelerate the water splitting reaction. When a water cluster or monolayer is formed on metal oxide, the LUMO or conduction band is contributed by the solvated electron state (also called a wet electron state) stabilized by the dangling H atoms [43]. Their energies distinctly depend on the network structure of these dangling H atoms. If such states can be stabilized to lower energy, they are able to accept the hot electrons from the metal clusters [44,45]. These findings shed light into the water splitting mechanism based on QWSs of metal clusters and provide an impetus for photoreactions in a wide range of applications.

[1] A. Fujishima and K. Honda, Nature (London) **238**, 37 (1972).

[2] X. Yang, A. Wolcott, G. Wang, A. Sobo, R. C. Fitzmorris, F. Qian, J. Z. Zhang, and Y. Li, Nano Lett. **9**, 2331 (2009).

[3] K. Maeda, T. Takata, M. Hara, N. Saito, Y. Inoue, H. Kobayashi, and K. Domen, J. Am. Chem. Soc. **127**, 8286 (2005).

[4] Q. Yan, J. Yu, S. K. Suram, L. Zhou, A. Shindec, P. F. Newhouse, W. Chen, G. Li, K. A. Persson, J. M. Gregoire, and J. B. Neaton, Proc. Natl. Acad. Sci. USA **114**, 3041 (2017).

[5] H. J. Shin, J. Jung, K. Motobayashi, S. Yanagisawa, Y. Morikawa, Y. Kim, and M. Kawai, Nat. Mater. **9**, 442 (2010).

[6] M. Haruta, T. Kobayashi, H. Sano, and N. Yamada, Chem. Lett. **16**, 405 (1987).

[7] B. Yoon, H. Hakkinen, U. Landman, A. S. Worz, J. M. Antonietti, S. Abbet, K. Judai, and U. Heiz, Science **307**, 403 (2005).

[8] M. Arenz, U. Landman, and U. Heiz, Chem. Phys. Chem. **7**, 1871 (2006).

[9] G. J. Hutchings and M. Haruta, Appl. Catal. A **291**, 2 (2005).

[10] G. J. Hutchings, J. Catal. **96**, 292 (1985).

[11] B. Nkosi, M. D. Adams, N. J. Coville, and G. J. Hutchings, J. Catal. **128**, 378 (1991).

[12] F. Boccuzzia, A. Chiorinoa, M. Manzolia, D. Andreevab, and T. Tabakovab, J. Catal. **188**, 176 (1999).

[13] S. Linic, P. Christopher, and D. B. Ingram, Nat. Mater. **10**, 911 (2011).

[14] T. Olsen and J. Schiøtz, Phys. Rev. Lett. **103**, 238301 (2009).

[15] S. V. Awate, S. S. Deshpande, K. Rakesh, P. Dhanasekaran, and N. M. Gupta, Phys. Chem. Chem. Phys. **13**, 11329 (2011).

[16] Z. Liu, W. Hou, P. Pavaskar, M. Aykol, and S. B. Cronin, Nano Lett. **11**, 1111 (2011).

[17] R. Boppella, S. T. Kochuveedu, H. Kim, M. J. Jeong, F. M. Mota, J. H. Park, and D. H. Kim, ACS Appl. Mater. Interfaces **9**, 7075 (2017).

[18] D. Ricci, A. Bongiorno, G. Pacchioni, and U. Landman, Phys. Rev. Lett. **97**, 036106 (2004).

[19] X. Lin, N. Nilius, H. J. Freund, M. Walter, P. Frondelius, K. Honkala, and H. Hakkinen, Phys. Rev. Lett. **102**, 206801 (2009).

[20] Z. Ding and S. Meng, Phys. Rev. B **86**, 045455 (2012).

[21] C. Zhang, B. Yoon, and U. Landman, J. Am. Chem. Soc. **129**, 2228 (2007).

[22] W. Kohn and L. J. Sham, Phys. Rev. **140**, A1133 (1965).

[23] D. Vanderbilt, Phys. Rev. B **41**, 7892 (1990).

[24] P. E. Blöchl, Phys. Rev. B **50**, 17953 (1994).

[25] J. P. Perdew, K. Burke, and M. Ernzerhof, Phys. Rev. Lett. **77**, 3865 (1996).

[26] G. Kresse and J. Hafner, Phys. Rev. B **47**, 558 (1993).

[27] G. Henkelman, B. P. Uberuaga, and H. Jónsson, J. Chem. Phys. **113**, 9901 (2000).

[28] W. R. Duncan, C. F. Craig, and O. V. Prezhdo, J. Am. Chem. Soc. **129**, 8528 (2007).

[29] Z. Li, X. Zhang, and G. Lu, J. Phys. Chem. B **114**, 17077 (2010).

[30] J. C. Tully, J. Chem. Phys. **93**, 1061 (1990).

[31] K. Drukker, J. Comput. Phys. **153**, 225 (1999).

[32] J. C. Idrobo, W. Walkosz, S. F. Yip, S. Öğüt, J. Wang, and J. Jellinek, Phys. Rev. B **76**, 205422 (2007).

[33] L. Ferrighi, B. Hammer, and G. K. H. Madsen, J. Am. Chem. Soc. **131**, 10605 (2009).

[34] X. L. Hu, J. Carrasco, J. Klimeš, and A. Michaelides, Phys. Chem. Chem. Phys. **13**, 12447 (2011).

[35] P. Ganesh, P. R. C. Kent, and G. M. Veith, J. Phys. Chem. Lett. **2**, 2918 (2011).

[36] C. J. Karwacki, P. Ganesh, P. R. C. Kent, W. O. Gordon, G. W. Peterson, J. J. Niu, and Y. Gogotsi, J. Mater. Chem. A **1**, 6051 (2013).

[37] W. Tang, E. Sanville, and G. Henkelman, J. Phys.: Condens. Matter **21**, 084204 (2009).

[38] J. Jung, H. J. Shin, Y. Kim, and M. Kawai, Phys. Rev. B **82**, 085413 (2010).

[39] L. Yan, F. W. Wang, and S. Meng, ACS Nano **10**, 5452 (2016).

[40] Y. Nishijima, K. Ueno, Y. Kotake, K. Murakoshi, H. Inoue, and H. Misawa, J. Phys. Chem. Lett. **3**, 1248 (2012).

[41] Z. Ding, S. W. Gao, and S. Meng, New J. Phys. **17**, 013023 (2015).

[42] X. L. Hu, J. Klimeš, and A. Michaelides, Phys. Chem. Chem. Phys. **12**, 3953 (2010).

[43] K. Onda, B. Li, J. Zhao, K. D. Jordan, J. Yang, and H. Petek, Science **308**, 1154 (2005).

[44] J. Zhao, B. Li, K. D. Jordan, J. Yang, and H. Petek, Phys. Rev. B **73**, 195309 (2006).

[45] J. Zhao, B. Li, K. Onda, M. Feng, and H. Petek, Chem. Rev. **106**, 4402 (2006).